Measurements of CO in the upper troposphere and lower stratosphere

R.L. Herman [a,*], C.R. Webster [a], R.D. May [a], D.C. Scott [a], H. Hu [a], E.J Moyer [b],
P.O. Wennberg [b], T.F. Hanisco [c], E.J. Lanzendorf [c], R.J. Salawitch [a], Y.L. Yung [b],
J.J. Margitan [a], T.P. Bui [d]

[a] *Jet Propulsion Laboratory, California Institute of Technology, Pasadena, CA 91109, USA*
[b] *Division of Geological and Planetary Sciences, California Institute of Technology, Pasadena, CA 91125, USA*
[c] *Atmospheric Research Project, Harvard University, Cambridge, MA 02138, USA*
[d] *NASA Ames Research Center, Moffett Field, CA 94035, USA*

Importance of this Paper: The atmospheric distribution of CO can be used to constrain both transport and photochemistry in the upper troposphere and lower stratosphere. We have collected new in situ measurements of atmospheric CO at high altitude, up to 21 km, throughout the Northern Hemisphere and in the tropics. We accurately simulate tropical stratospheric CO using measured OH and modeled ascent rates, implying that all three are consistent. The Northern Hemisphere seasonal distribution of CO betwen 7 and 21 km altitude is drawn on contour maps for intercomparison with global atmospheric models and satellite measurements.

Abstract

In situ measurements of CO were made in the upper troposphere and lower stratosphere (7–21 km altitude) with the Jet Propulsion Laboratory (JPL) Aircraft Laser Infrared Absorption Spectrometer (ALIAS) on 58 flights of the NASA ER-2 aircraft from October 1995 through September 1997, between 90°N and 3°S latitude. Measured upper tropospheric CO was variable and typically ranged between 55 and 115 ppb, except for higher values over Alaska during summer 1997. Tropical stratospheric CO ranged from 58 ± 5 ppb at the tropopause to 12 ± 2 ppb above 20 km, having similar profiles in all seasons of the year. The tropical profile is reproduced by a simple Lagrangian box model of tropical ascent using measured CH_4 and OH concentrations, Cl and $O(^1D)$ concentrations from a photochemical model, and diabatic heating rates from a radiative heating model. From measured CO, quasi-horizontal mixing between the tropical and mid-latitude lower stratosphere is inferred to be rapid in the region between 400 K and 450 K potential temperature (altitudes less than 20 km). © 1999 Elsevier Science Ltd. All rights reserved.

Keywords: Carbon monoxide; In situ measurement; Upper troposphere; Lower stratosphere

* Corresponding author. Present address: Mail Stop 183-401, Jet Propulsion Laboratory, 4800 Oak Grove Drive, Pasadena, CA91109, USA. E-mail: rherman@igor.jpl.nasa.gov

1. Introduction

Carbon monoxide (CO) plays a central role in atmospheric photochemistry (e.g., Logan et al., 1981; Crutzen, 1995). It has been recognized that CO is the dominant sink of tropospheric OH, the primary oxidant in the troposphere (Levy, 1971). CO also contributes to O_3 production in the troposphere (e.g., Fishman and Crutzen, 1978; Seiler and Fishman, 1981), and potentially in the lowermost stratosphere as well (Bregman et al., 1997). In the troposphere, the dominant sources of CO are oxidation of CH_4 and other hydrocarbons, biomass burning, and direct anthropogenic emissions (e.g., Logan et al., 1981). In the lowermost stratosphere, the dominant source of CO is transport from the CO-rich boundary layer (e.g., Harriss et al., 1992, 1994), but at higher altitudes the dominant source is local production from CH_4 oxidation (e.g., Logan et al., 1981; Pinto et al., 1983). CO is the longest-lived intermediate in the oxidation pathway from CH_4 to CO_2, which is initiated by:

$$CH_4 + X \rightarrow CH_3 + HX,$$
$$\text{where } X = OH, O(^1D), \quad (1)$$
$$\text{or Cl}; X = OH \text{ dominant.}$$
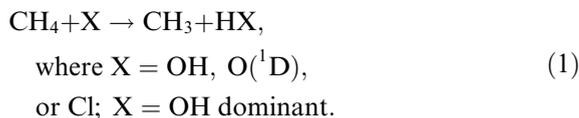
Reaction (1) is the rate-limiting step in CO production from CH_4, and has a strong temperature-dependence for $X = OH$ or Cl. Subsequent photochemical reactions rapidly produce CH_2O, which is photolyzed to CO.

The lifetime of CO with respect to photochemical loss is controlled by reaction with OH (Pressman and Warneck, 1970; Logan et al., 1981):

$$CO + OH \rightarrow CO_2 + H. \quad (2)$$

In the lower stratosphere, the CO mixing ratio is much greater than its steady-state value due to transport across the tropopause. As air ascends in the tropical stratosphere, CO decreases exponentially due to reaction (2) until photochemical steady state is reached.

Aircraft in situ measurements of atmospheric CO have the potential to improve our understanding of rapid transport within the lower stratosphere because CO has a photochemical lifetime of only three months. Aircraft measurements have excellent vertical resolution of the near-tropopause region compared to remote sensing observations (e.g., Gunson et al., 1996), and wide enough spatial coverage to carry out studies on regional to hemispheric scales. There have been numerous in situ aircraft studies of CO up to 12.5 km altitude (e.g., Seiler and Fishman, 1981; Robinson et al., 1984; Marenco et al., 1989; Harriss et al., 1992; Anderson et al., 1993; Harriss et al., 1994; Roths and Harris, 1996; Ridley et al., 1997; Lelieveld et al., 1997; Waibel et al., 1998; Hoor et al., 1999). However, the NASA ER-2 aircraft has made possible measurements at altitudes up to 21 km (e.g., Hipskind et al., 1987; Murphy et al., 1993). The ER-2 database is unique in the large number of trace gases that are measured simultaneously with particle concentration, solar irradiance, and meteorological variables (e.g., Tuck et al., 1997). Aboard the ER-2, the Aircraft Laser Infrared Absorption Spectrometer (ALIAS) of the Jet Propulsion Laboratory (JPL) measures CO, N_2O, CH_4 and HCl concentrations with high precision and accuracy (see below) and a rapid 3 s response time (Webster et al., 1994). In 1995–1997, ALIAS collected data on 58 flights of the ER-2 during two NASA campaigns: Stratospheric TRacers of Atmospheric Transport (STRAT) in 1995–1996 and Photochemistry of Ozone Loss in the Arctic Region In Summer (POLARIS) in 1997. This paper describes the spatial distribution of upper tropospheric and lower stratospheric CO measured by ALIAS on those campaigns. In addition, simultaneous in situ measurements of OH (Wennberg et al., 1994) and a simple model are used to constrain the CO photochemical lifetime, evaluate our understanding of ascent in the tropical lower stratosphere, and estimate quasi-horizontal transport time scales in the lower stratosphere.

2. Aircraft instruments

ALIAS is a high-resolution, scanning, mid-infrared absorption spectrometer that has four tun-

able diode lasers (TDLs) to simultaneously measure CO, N_2O, CH_4 and HCl concentrations (May and Webster, 1993; Webster et al., 1994). The instrument achieves high sensitivity by using harmonic spectroscopy: absorptions as small as 1 part in 10^5 can be detected in a 3 s integration period. The signal is amplified, filtered, and demodulated at twice the laser modulation frequency to yield second-harmonic spectra. Each of the four channels has an InSb or HgCdTe detector mounted inside the same liquid nitrogen Dewar as the TDLs. Thirty spectral scans are averaged together and written to a hard disk every 3 s along with engineering data such as laser power, detector zero level, pressure, gas temperature, component temperatures and heater powers.

The instrument is mounted in a pod on the right wing of the ER-2. At atmospheric pressures less than 500 hPa, an inlet wheel is opened to allow sampling. Air enters a heated inlet probe in front of the wing pod and flows through a 1 m absorption cell with a flush time of 1–2 s. The 3 s instrument response time allows measurements with high spatial resolution along the flight path of the aircraft ($\approx$600 m horizontal resolution, 50 m vertical resolution). Within the absorption cell, the infrared laser beams are reflected 80 times between two Au-coated spherical aluminum mirrors in a Herriott cell multipass optical configuration to achieve a 80 m optical pathlength. For CO, the instrument precision ($\pm$1 standard deviation) is $\pm$0.7 parts per billion by volume (ppb) for 3 s average data. For ground calibration, we use gas standards provided by the National Oceanic and Atmospheric Administration (NOAA) Climate Monitoring and Diagnostics Laboratory (CMDL). The calibration gases are introduced into the absorption cell and spectra are taken over the range of pressures expected during flight. The estimated instrument accuracy ($\pm$1 standard deviation) is $\pm$5% relative to these calibration standards.

In the following analysis, we use simultaneous measurements of CO, CH_4, OH, H_2O and O_3 concentrations, temperature, pressure and tropopause height obtained aboard the ER-2. The Harvard HO_x instrument uses laser-induced fluorescence to measure OH concentrations (Wennberg et al., 1994). H_2O concentrations are measured by the Harvard H_2O instrument with Lyman-α photofragment fluorescence (Weinstock et al., 1994) and also by the JPL H_2O instrument using near-infrared TDL spectroscopy (May, 1998). The NOAA O_3 instrument measures O_3 concentrations by ultraviolet absorption spectroscopy (Proffitt and McLaughlin, 1983). Temperature and pressure are measured by the ER-2 Meteorological Measurement System (MMS) (Scott et al., 1990). The JPL Microwave Temperature Profiler (MTP) is a passive microwave radiometer that determines the local temperature profile by measuring O_2 thermal emission at different elevation angles (Denning et al., 1989). The local tropopause height is inferred from the MMS and MTP temperature profiles (B.L. Gary, 1998, personal communication).

3. CO distribution

ALIAS has measured CO in the upper troposphere and lower stratosphere between 7 and 21 km altitude during the STRAT and POLARIS campaigns in 1995–1997. In the upper troposphere, the abundance of CO varies considerably on daily to seasonal time scales (e.g., Logan et al., 1981). Fig. 1 shows monthly distributions of upper tropospheric CO measured at three latitudes: 65°N near Fairbanks, Alaska (11 flights); 37°N near NASA Ames Research Center, Moffett Field, California (17 flights); and 21°N near Barber's Point, Hawaii (20 flights). Data included in this figure are limited to altitudes between 7 km and the local tropopause −1 km. Generally, CO mixing ratios are lower in the upper troposphere than at surface stations because CO is dominantly produced in the boundary layer (e.g., Logan et al., 1981). Since the instrument precision is $\pm$0.7 ppb CO, the scatter within each month of data reflects true atmospheric variability. Fig. 1 indicates that upper tropospheric CO mixing ratios are generally greater at higher latitudes in the Northern Hemisphere, similar to previous observations (e.g., Seiler and Fishman, 1981; Robinson et al., 1984; Marenco et al., 1989; Anderson et al., 1993; Roths and Harris, 1996).
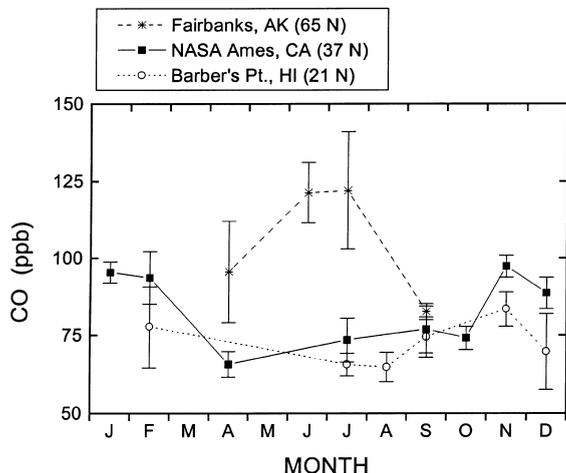
Fig. 1. Upper tropospheric CO measured by ALIAS between 7 km altitude and the local tropopause −1 km. Symbols are monthly means (±1 standard deviation). Instrument precision is ±0.7 ppb, so the observed scatter within each monthly bin is evidence of atmospheric variability. These tropospheric data are from 11 flights at 65°N, 17 flights at 37°N and 20 flights at 21°N.

The striking summer maximum of upper tropospheric CO over Alaska (Fig. 1) is caused by convection, most likely due to forest fires (e.g., Harriss et al., 1992, 1994; Yurganov et al., 1998; Waibel et al., 1998). The June and July data are similar to mean tropospheric CO mixing ratios expected in high latitude air contaminated by forest fires (Yurganov et al., 1998). Such high mixing ratios of CO may lead to significant O_3 production in the upper troposphere (Fishman and Crutzen, 1978). Given the small number of high latitude flights with tropospheric data, the monthly mean mixing ratios are very uncertain. Nevertheless, the summer mixing ratios are by far the highest observed.

At mid-latitudes (37°N, California), upper tropospheric CO has an annual maximum of 85–100 ppb in late autumn and winter, and a minimum of 60–70 ppb in spring (Fig. 1). In the subtropics (21°N, Hawaii), upper tropospheric CO has a similar seasonal cycle with an annual maximum of 80–90 ppb and a minimum of 60–70 ppb. Note that the greatest variability in subtropical CO is seen in late autumn to winter (December and February). At both latitudes, synoptic-scale

dynamics and stratosphere-troposphere exchange produce variability in CO on time scales of days to weeks.

Tropical CO profiles have been measured by ALIAS on five flights from Hawaii to the equatorial central Pacific Ocean (10°N–3°S, 150°W–160°W), as shown in Fig. 2. Near the equator, the aircraft descends from its cruise altitude of 21 km in the stratosphere to a minimum altitude of 15 km near the tropical tropopause, and then climbs back to 21 km. We find that CO is less variable in the tropics than at higher latitudes in the Northern Hemisphere. Between 15 km and the tropopause, the equatorial CO mixing ratio is 60 ± 5 ppb with no apparent seasonal variation. These mixing ra-
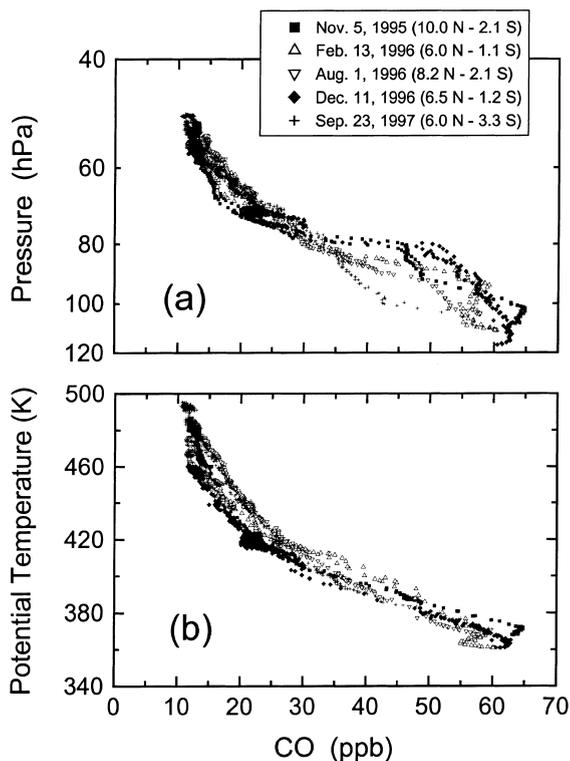

Fig. 2. Tropical CO profiles measured by ALIAS on five flights over the equatorial central Pacific Ocean (150°W–160°W, with latitude ranges shown in legend): (a) CO fluctuates as a function of pressure, depending on the height of the tropopause; (b) As a function of potential temperature θ, CO has nearly the same vertical profile throughout the year, with a tropical tropopause at 370 ± 10 K (≈15.5–17.2 km).

tios are slightly lower than tropical measurements at lower altitudes over the open Pacific, reflecting photochemical loss of CO in the upper troposphere (e.g., Gregory et al., 1997; Novelli et al., 1998).

In the tropical lower stratosphere, the CO mixing ratio decays with altitude due to photochemical loss. The vertical profile of CO is strongly affected by seasonal variations in tropopause height (Fig. 2a). However, the potential temperature of the tropical tropopause varies less than the altitude of the tropopause (Reid and Gage, 1996) (potential temperature is defined as the temperature of an air parcel adiabatically compressed or expanded to 1000 hPa). Potential temperature, θ, is a tracer of adiabatic motion and is conserved on time scales of approximately two weeks. The stratospheric CO profile in the equatorial central Pacific varies little with season if θ is used as the vertical coordinate (Fig. 2b). CO and θ are strongly anticorrelated in the tropical lower stratosphere because diabatic heating increases θ while photochemistry decreases the CO mixing ratio. The mean tropical tropopause for these five flights is at $\theta \approx 370 \pm 10$ K (altitudes ranging from 15.5 to 17.2 km) with a corresponding CO mixing ratio of 58 ± 5 ppb. By $\theta = 390$ K, tropical air has CO abundances of only 45 ± 5 ppb. The lowest mixing ratios of CO measured by ALIAS in the tropics are 12 ± 2 ppb at altitudes above 20 km ($\theta > 470$ K). Weinstock et al. (1999) has used the functional relationship between CO and θ as a photochemical clock to infer the stratospheric age of air parcels. In the following Analysis section, we will demonstrate that the loss of tropical CO is consistent with measured concentrations of OH, rate coefficients for (1) and (2), and calculated heating rates.

The tropical correlation plot of O_3 vs. CO measured over the equatorial central Pacific (10°N–3°S, 150–160°W) is shown in Fig. 3. Tropical stratospheric O_3 and CO are anticorrelated due to local photochemical production of O_3 and destruction of CO (e.g., Avallone and Prather, 1996). This correlation is in excellent quantitative agreement with previous measurements made during the Stratospheric Tropospheric Exchange Program (STEP) near Darwin, Australia (Fig. 12
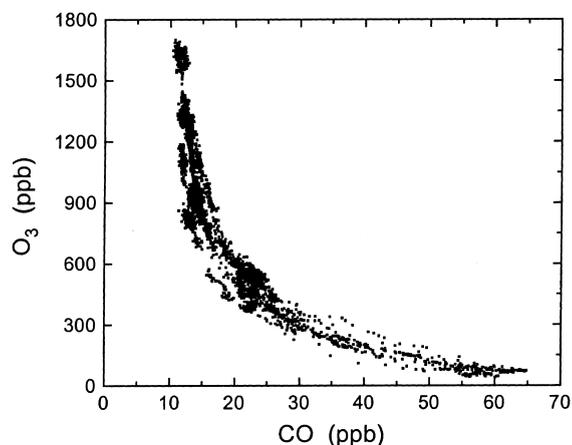

Fig. 3. Tropical O_3 vs. CO measured over the equatorial central Pacific (flight dates and latitude ranges are same as in Fig. 2).

of Murphy et al., 1993; Fig. 2 of Avallone and Prather, 1996), and appears to be a robust feature of the tropical stratosphere.

ALIAS made extensive measurements of stratospheric CO on 58 flights up to 21 km altitude at latitudes ranging from 90°N to 3°S in 1995–1997. This database is extensive enough to map the seasonal distributions of CO in the Northern Hemisphere upper troposphere and lower stratosphere, as shown in Fig. 4. Each contour plot uses data from at least 15 flights, binned in increments of 20° latitude, 0.5 km altitude, and 10 K potential temperature. For altitudes below 15 km, data are limited to the vicinities of the landing bases at 21°N, 37°N and 65°N. Superimposed on Fig. 4 are the seasonal means (open squares) of the tropopause heights measured on the same ER-2 flights. The location of the tropopause shifts from day to day, so the CO gradient across the tropopause is smoothed by the contour plots. Nevertheless, this is a unique database for comparison with atmospheric models. Figs. 4a,c and e, use pressure altitude as the vertical coordinate. The summer maximum of CO at high latitudes in the upper troposphere is seen clearly in Fig. 4c. In the stratosphere, isopleths of constant CO mixing ratio slope downward toward the pole as expected from the Brewer–Dobson circulation model (Brewer, 1949; Dobson, 1956).
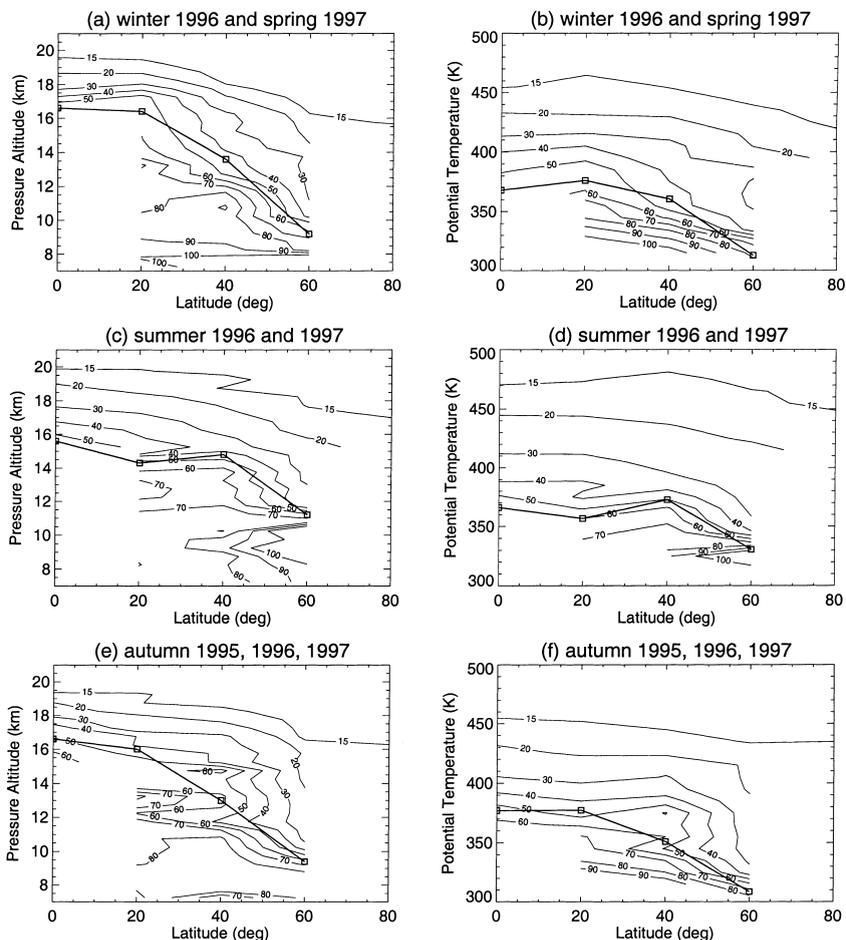
Fig. 4. ALIAS CO distribution (ppb) in the upper troposphere and lower stratosphere of the Northern Hemisphere. Superimposed on the plots are the seasonal means (open squares) of the tropopause heights measured on the same ER-2 flights. These plots represent seasonal averages created by binning the data every 20° latitude and 0.5 km altitude (or 10 K potential temperature): (a) winter 1996 and spring 1997 altitude vs. latitude (15 flights); (b) winter 1996 and spring 1997 potential temperature vs. latitude (15 flights); (c) summer 1996 and 1997 altitude vs. latitude (21 flights); (d) summer 1996 and 1997 potential temperature vs. latitude (21 flights); (e) autumn 1995, 1996 and 1997 altitude vs. latitude (21 flights); (f) autumn 1995, 1996 and 1997 altitude vs. latitude (21 flights).

To remove transient motions that produce no net vertical transport, potential temperature θ is used as the vertical coordinate in Figs. 4b,d and f. It is immediately apparent that the CO isopleths are flatter in θ than in altitude. The stratosphere can be divided into two layers: the "overworld" ($\theta > 380$ K), and the stratospheric "middleworld" (bounded above by the $\theta = 380$ K isentrope and below by the extra-tropical tropopause) (Hoskins, 1991; Holton et al., 1995). In the stratospheric middleworld, there is considerable variability in CO due to stratosphere–troposphere exchange at a wide range of latitudes, similar to previous observations (e.g., Lelieveld et al., 1997). CO is less variable in the overworld than in the middleworld, although the 15 and 20 ppb isopleths are displaced to higher θ in summer due to greater production from CH_4 oxidation. CO isopleths are flatter in the overworld than in the middleworld, especially for 400 K $< \theta <$ 450 K between 0°N and 40°N. In the

Analysis section, we will infer transport rates within the lower stratosphere from the CO distribution in the overworld.

4. Analysis

We will first examine vertical transport in the tropical stratosphere using a simple Lagrangian photochemical box model of tropical ascent. The model includes diabatic heating and photochemical production and loss of CO:

$$Q(\partial\chi/\partial\theta) = -L\chi + P, \tag{3}$$

where Q is the diabatic heating rate (equivalent to ascent rate in isentropic coordinates), χ is the CO concentration, loss $L = k_2[OH]$, production P is the rate of (1), and each term is parameterized as a function of potential temperature θ (using the annual mean tropical relationship between θ and pressure). Q is the mass-balanced, annual mean tropical heating rate calculated from a radiative heating model, with typical uncertainties of $\pm 60\%$ at pressures greater than 50 hPa (Rosenlof, 1995). Reaction rate coefficients are from DeMore et al. (1997). In the tropical lower stratosphere, measured OH is not strongly dependent on altitude (Fig. 5). A quadratic fit of tropical OH data to solar zenith angle is used to calculate a 24 h mean OH concentration of $8 \pm 3 \times 10^5$ cm^{-3} for the tropical lower stratosphere, which corresponds to a CO photochemical lifetime of 100 ± 40 days. 24 h mean concentrations of Cl and O(^{1}D) are calculated with a photochemical model (Salawitch et al., 1994) constrained by tropical measurements of H$_2$O, CH$_4$, O$_3$, NO$_y$, Cl$_y$, and particle surface area (e.g., Herman et al., 1998). The annual mean calculated reaction rates are shown in Fig. 6.

The tropical model is in excellent agreement with stratospheric CO measurements using a boundary condition of 58 ppb CO at $\theta = 370$ K (Fig. 7). Such good agreement indicates a high level of consistency among measured CO and OH concentrations, rate coefficients, and diabatic heating rates. This is noteworthy because the model results are sensitive to changes in each input
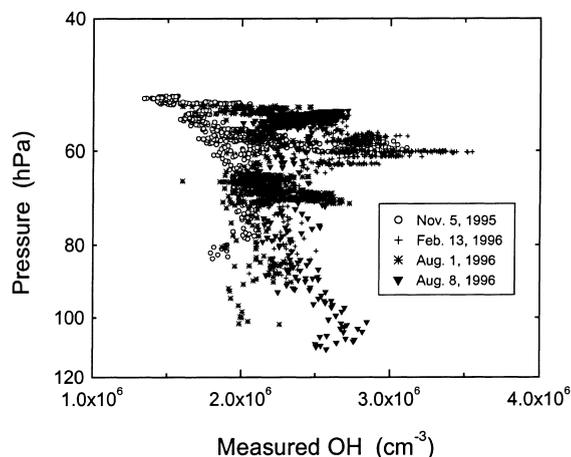

Fig. 5. Tropical stratospheric OH measured by the Harvard HO$_x$ instrument aboard the ER-2. Flight dates and latitude ranges are the same as in Fig. 2, except for the flight of August 8, 1996 (5°N–10°N).
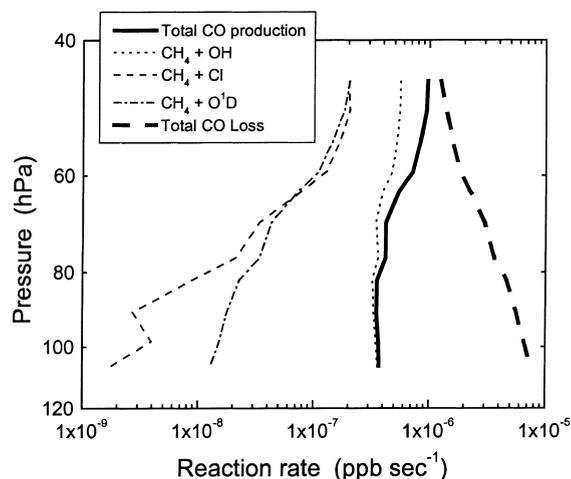

Fig. 6. Annual average CO production and loss rates in the tropics. The rates were calculated from mean measured profiles of CO and CH$_4$, 24 h mean profiles of Cl and O(^{1}D) from a photochemical model (Salawitch et al., 1994) and 24 h mean OH concentration (8×10^5 cm^{-3}) inferred from an empirical relationship between measured OH and solar zenith angle.

term, as shown in Fig. 7. The scatter in the observed CO is much smaller than the error expected in the model calculation, especially for $\theta > 420$ K. Either some uncertainties have been overestimated
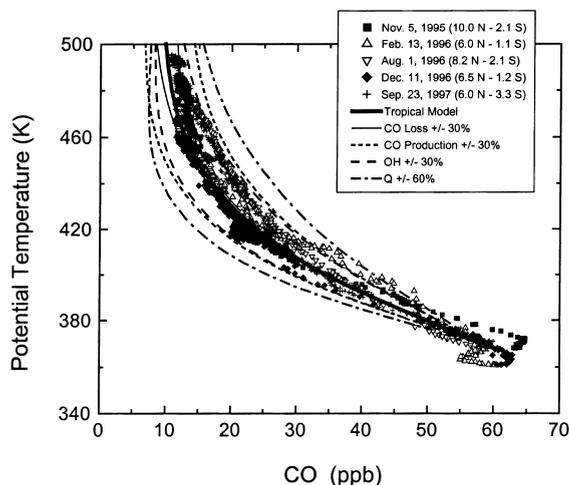
Fig. 7. Measured tropical CO profiles (same as Fig. 2b) and predicted CO profiles from the Lagrangian box model. The model is in excellent agreement with the data despite its sensitivity to input parameters.

Fig. 8. Measured CO is highly correlated with N_2O on a constant-altitude flight leg (14.9 km, 122–123 hPa, $380 < \theta < 385$ K) during 29 January, 1996, mid-latitude flight of the ER-2 (solid squares). On the other mid-latitude flights, a significantly different relationship is seen (open circles ±1 standard deviation). The linearity of 29 January, 1996, data suggests a mixing line between the tropics (52 ppb CO, 315 ppb N_2O) and mid-latitudes (13.5 ppb CO, 260 ppb N_2O).

or covariance between terms reduces some of the total uncertainty in the model.

Horizontal transport in the stratosphere can also be examined by looking at the CO distribution. In Fig. 4, the flat isopleths of CO in the overworld suggest that quasi-horizontal mixing is fast relative to photochemical loss of CO at altitudes below 20 km. We will now look at this phenomenon in greater detail. During the 29 January, 1996, mid-latitude flight of the ER-2, there was a constant-altitude flight leg at 14.9 km (380 K $< \theta <$ 385 K) with H_2O mixing ratios less than 4 parts per million. Air this dry must have entered the stratosphere at the tropical tropopause (Hintsa et al., 1994). ALIAS measured highly correlated mixing ratios of CO and N_2O on this flight leg, as shown in Fig. 8. The 29 January CO and N_2O data are significantly different from the other mid-latitude data (open circles) and appear to form a mixing line (dashed line). The data with the greatest tropical character have approximately 41 ppb CO and 300 ppb N_2O at $\theta = 381$ K. Extrapolating to the tropical end-member (315 ppb N_2O) yields 52 ppb CO. At 14.9 km altitude, local photochemical loss of N_2O is negligible, so this air parcel is a mixture of young tropical air and photochemically aged mid-latitude air which has
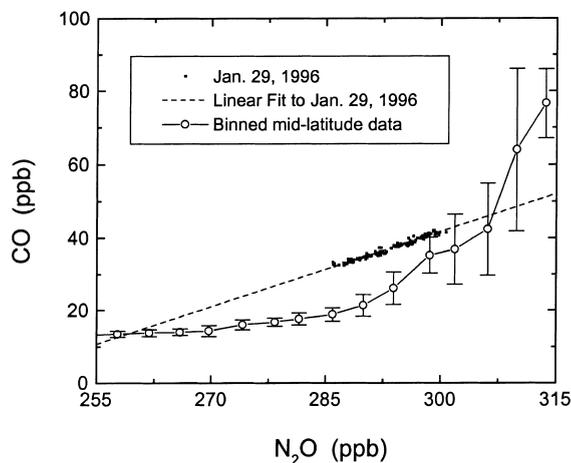
been transported through the stratosphere by the Brewer–Dobson circulation. The end-member CO mixing ratio (52 ppb) is very similar to tropical values observed on the 381 K isentropic surface (49.5 ± 2 ppb), indicating that transport out of the tropics was sufficiently rapid to avoid significant photochemical loss of CO.

We can generalize about quasi-horizontal transport in the lower stratosphere by comparing annual and seasonal mean CO profiles at different latitudes. Fig. 9 shows mean stratospheric CO profiles for the annual mean, winter, and summer (binned by θ and latitude as in Fig. 4). The mid-latitude and tropical profiles are very similar because poleward transport is rapid relative to the CO photochemical lifetime. The difference between mid-latitude and tropical CO at constant θ corresponds to a chemical loss time scale of less than one month for 400 K $< \theta <$ 450 K. This time scale is shorter than independent estimates for quasi-horizontal transport from tropics to mid-latitudes (e.g., Boering et al., 1995; Boering et al., 1996; Hintsa et al., 1994), and suggests that not all of the transport is adiabatic. Considering the large
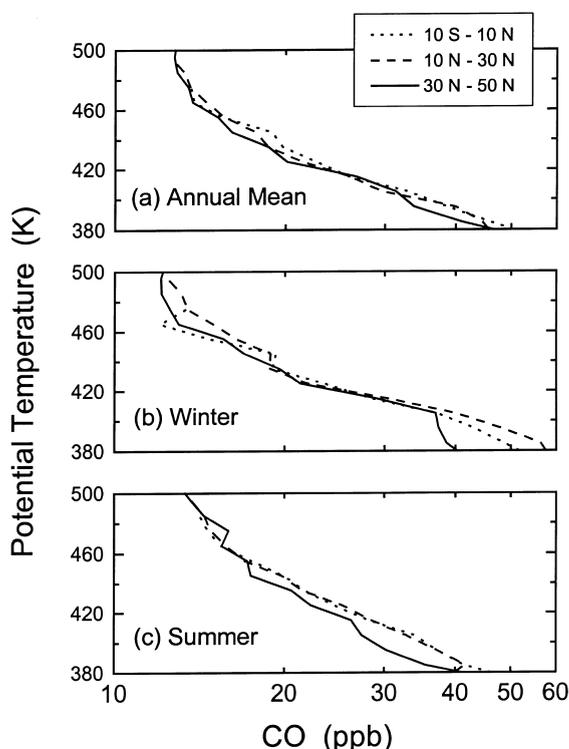
Fig. 9. Mean profiles of measured CO in the stratospheric overworld, binned by latitude and potential temperature: (a) annual mean (57 flights); (b) winter (7 flights); (c) summer (21 flights). The similarity of these profiles suggests that quasi-horizontal transport is rapid in the lower stratosphere.

vertical gradient of CO, vertical eddy diffusion probably plays a significant role. The tropical and mid-latitude CO profiles are more similar in winter than in summer, which is consistent with faster quasi-horizontal mixing in winter (e.g., Chen et al., 1994; Waugh, 1996).

5. Summary

In this paper, we have described the distribution of CO in the upper troposphere and lower stratosphere measured by ALIAS from October 1995 through September 1997. In the upper troposphere, CO has a seasonal cycle with a maximum in autumn and winter, and a minimum in spring and summer. During summer in Alaska,

however, upper tropospheric CO is elevated due to convection possibly associated with forest fires. Over the equatorial central Pacific, upper tropospheric CO mixing ratios are 60 ± 5 ppb with little seasonal variation. In the tropical lower stratosphere, CO decreases as potential temperature increases, with little seasonal variation. The tropical stratospheric correlations of CO with θ and with O_3 appear to be robust features of the atmosphere.

A simple Lagrangian box model reproduces the measured tropical profile of CO with a high degree of accuracy, demonstrating a strong level of consistency between measured concentrations of CO and OH, rate coefficients for reactions (1) and (2), and calculated diabatic heating rates. Contour plots of CO have flat isopleths at potential temperatures between 400 and 450 K (altitudes below 20 km) due to rapid transport from the tropics to the mid-latitude stratosphere. Since this air has only recently entered the stratosphere, it has relatively large concentrations of CO and potentially other reactive species that could affect mid-latitude stratospheric O_3 abundances.

References

Anderson, B.E., Collins, J.E., Sachse, G.W., Whiting, G.W., Blake, D.R., Rowland, F.S., 1993. AASE-II Observations of trace carbon species distributions in the mid to upper troposphere. Geophys. Res. Lett. 20, 2539–2542.

Avallone, L.M., Prather, M.J., 1996. Photochemical evolution of ozone in the lower tropical stratosphere. J. Geophys. Res. 101, 1457–1461.

Boering, K.A., Hintsa, E.J., Wofsy, S.C., Anderson, J.G., Daube Jr, B.C., Dessler, A.E., Loewenstein, M., McCormick, M.P., Podolske, J.R., Weinstock, E.M., Yue, G.K., 1995. Measurements of stratospheric carbon dioxide and water vapor at northern midlatitudes: Implications for troposphere-to-stratosphere transport. Geophys. Res. Lett. 22, 2737–2740.

Boering, K.A., Wofsy, S.C., Daube, B.C., Schneider, H.R., Loewenstein, M., Podolske, J.R., Conway, T.J., 1996. Stratospheric mean ages and transport rates from observations of carbon dioxide and nitrous oxide. Science 274, 1340–1343.

Bregman, A., Arnold, F., Bürger, V., Fischer, H., Lelieveld, J., Scheeren, B.A., Schneider, J., Siegmund, P.C., Ström, J., Waibel, A., Wauben, W.M.F., 1997. In situ trace gas and particle measurements in the summer lower stratosphere during STREAM II: implications for O_3 production. J. Atmos. Chem. 26, 275–310.

Brewer, A.W., 1949. Evidence for a world circulation provided by the measurements of helium and water vapor distribution in the stratosphere. Q. J. Roy. Meteor. Soc. 75, 351–363.

Chen, P., Holton, J.R., O'Neill, A., Swinbank, R., 1994. Isentropic mass exchange between the tropics and extratropics in the stratosphere. J. Atmos. Sci. 51, 3006–3018.

Crutzen, P.J., 1995. Ozone in the troposphere, Chapter 10. In: Singh, H.B. (Ed.), Composition, Chemistry, and Climate of the Atmosphere, Van Nostrand Reinhold, New York, pp. 349–393.

DeMore, W.B., Sander, S.P., Golden, D.M., Hampson, R.F., Kurylo, M.J., Howard, C.J., Ravishankara, A.R., Kolb, C.E., Molina, M.J., 1997. Chemical Kinetics and Photochemical Data for Use in Stratospheric Modeling. JPL Publication 97-4, Jet Propulsion Laboratory, Pasadena, CA.

Denning, R.F., Guidero, S.L., Parks, G.S., Gary, B.L., 1989. Instrument description of the airborne microwave temperature profiler. J. Geophys. Res. 94, 16757–16765.

Dobson, G.M.B., 1956. Origin and distribution of the polyatomic molecules in the atmosphere. Proc. Roy. Soc. London A 236, 187–193.

Fishman, J., Crutzen, P.J., 1978. The origin of ozone in the troposphere. Nature 274, 855–858.

Gregory, G.L., Merrill, J.T., Shipham, M.C., Blake, D.R., Sachse, G.W., Singh, H.B., 1997. Chemical characteristics of tropospheric air over the pacific ocean as measured during PEM-West B: Relationship to Asian outflow and trajectory history. J. Geophys. Res. 102, 28275–28285.

Gunson, M.R., Abbas, M.M., Abrams, M.C., Allen, M., Brown, L.R., Brown, T.L., Chang, A.Y., Goldman, A., Irion, F.W., Lowes, L.L., Mahieu, E., Manney, G.L., Michelsen, H.A., Newchurch, M.J., Rinsland, C.P., Salawitch, R.J., Stiller, G.P., Toon, G.C., Yung, Y.L., Zander, R., 1996. The atmospheric trace molecule spectroscopy (ATMOS) experiment: deployment on the ATLAS space shuttle missions. Geophys. Res. Lett. 23, 2333–2336.

Harriss, R.C., Sachse, G.W., Collins, J.E., Wade, L., Bartlett, K.B., Talbot, R.W., Browell, E.V., Barrie, L.A., Hill, G.F., Burney, L.G., 1994. Carbon monoxide and methane over Canada: July–August 1990. J. Geophys. Res. 99, 1659–1669.

Harriss, R.C., Sachse, G.W., Hill, G.F., Wade, L., Bartlett, K.B., Collins, J.E., Steele, L.P., Novelli, P.C., 1992. Carbon monoxide and methane in the north American arctic and subarctic: July–August. J. Geophys. Res. 97, 16589–16599.

Herman, R.L., Scott, D.C., Webster, C.R., May, R.D., Moyer, E.J., Salawitch, R.J., Yung, Y.L., Toon, G.C., Sen, B., Margitan, J.J., Rosenlof, K.H., Michelsen, H.A., Elkins, J.W., 1998. Tropical entrainment time scales inferred from stratospheric N_2O and CH_4 observations. Geophys. Res. Lett. 25, 2781–2784.

Hintsa, E.J., Weinstock, E.M., Dessler, A.E., Anderson, J.G., Loewenstein, M., Podolske, J.R., 1994. SPADE H_2O measurements and the seasonal cycle of stratospheric water vapor. Geophys. Res. Lett. 21, 2559–2562.

Hipskind, R.S., Gregory, G.L., Sachse, G.W., Hill, G.F., Danielson, E.F., 1987. Correlations between ozone and carbon monoxide in the lower stratosphere, folded tropopause, and maritime troposphere. J. Geophys. Res. 92, 2121–2130.

Holton, J.R., Haynes, P.H., McIntyre, M.E., Douglass, A.R., Rood, R.B., Pfister, L., 1995. Stratosphere–troposphere exchange. Rev. Geophys. 33, 403–439.

Hoor, P., Konigstedt, R., Parchtka, U., Wienhold, F.G., Fischer, H., 1999. Measurements of CO in the arctic lower stratosphere during winter. Chemosphere, in prep.

Hoskins, B.J., 1991. Towards a PV-theta view of the general circulation. Tellus, Ser. A. 43, 27–35.

Lelieveld, J., Bregman, B., Arnold, F., Bürger, V., Crutzen, P.J., Fischer, H., Waibel, A., Siegmund, P., Van Velthoven, P.F.J., 1997. Chemical perturbation of the lowermost stratosphere through exchange with the troposphere. Geophys. Res. Lett. 24, 603–606.

Levy, H., 1971. II Normal atmosphere: Large radical and formaldehyde concentrations predicted. Science 173, 141–143.

Logan, J.A., Prather, M.J., Wofsy, S.C., McElroy, M.B., 1981. Tropospheric chemistry: a global perspective. J. Geophys. Res. 86, 7210–7254.

Marenco, A., Macaigne, M., Prieur, S., 1989. Meridional and vertical CO and CH_4 distributions in the background troposphere (70°N–60°S; 0–12) km altitude from scientific aircraft measurements during the STRATOZ III experiment (June 1984). Atmos. Environ. 23, 185–200.

May, R.D., 1998. Open-path, near-infrared tunable diode laser spectrometer for atmospheric measurements of H_2O. J. Geophys. Res. 103, 19161–19172.

May, R.D., Webster, C.R., 1993. Data processing and calibration for tunable diode laser harmonic absorption spectrometers. J. Quant. Spectrosc. Radiat. Transfer 49, 335–347.

Murphy, D.M., Fahey, D.W., Proffitt, M.H., Liu, S.C., Chan, K.R., Eubank, E.S., Kawa, S.R., Kelly, K.K., 1993. Reactive nitrogen and its correlation with ozone in the lower stratosphere and upper troposphere. J. Geophys. Res. 98, 8751–8773.

Novelli, P.C., Masarie, K.A., Lang, P.M., 1998. Distributions and recent changes of carbon monoxide in the lower troposphere. J. Geophys. Res. 103, 19015–19033.

Pinto, J.P., Yung, Y.L., Rind, D., Russell, G.L., Lerner, J.A., Hansen, J.E., Hameed, S., 1983. A general circulation model study of atmospheric carbon monoxide. J. Geophys. Res. 88, 3691–3702.

Pressman, J., Warneck, P., 1970. The stratosphere as a chemical sink for carbon monoxide. J. Atm. Sci. 27, 155–163.

Proffitt, M.H., McLaughlin, R.J., 1983. Fast-response dual-beam UV-absorption ozone photometer suitable for use on stratospheric balloons. Rev. Sci. Instrum. 54, 1719–1728.

Reid, G.C., Gage, K.S., 1996. The tropical tropopause over the western Pacific: wave driving, convection, and the annual cycle. J. Geophys. Res. 101, 21233–21241.

Ridley, B.A., Atlas, E.L., Walega, J.G., Kok, G.L., Staffelbach, T.A., Greenberg, J.P., Grahek, F.E., Hess, P.G., Montzka, D.D., 1997. Aircraft measurements made during the spring maximum of ozone over Hawaii: peroxides CO, O_3, NO_y, condensation nuclei, selected hydrocarbons, halocarbons, and alkyl nitrates between 0.5 and 9 km altitude. J. Geophys. Res. 102, 18935–18961.

Robinson, E., Clark, D., Seiler, W., 1984. The latitudinal distribution of carbon monoxide across the pacific from california to antarctica. J. Atmos. Chem. 1, 137–149.

Rosenlof, K.H., 1995. Seasonal cycle of the residual mean meridional circulation in the stratosphere. J. Geophys. Res. 100, 5173–5191.

Roths, J., Harris, G.W., 1996. The tropospheric distribution of carbon monoxide as observed during the TROPOZ II experiment. J. Atmos. Chem. 24, 157–188.

Salawitch et al, R.J., 1994. The diurnal variation of hydrogen, nitrogen and chlorine radicals: implications for the heterogeneous production of HNO_2. Geophys. Res. Lett. 21, 2551–2554.

Scott, S.G., Bui, T.P., Chan, K.R., Bowen, S.W., 1990. The meteorological measurement system on the NASA ER-2 aircraft. J. Atmos. and Oceanic Technol. 7, 525–540.

Seiler, W., Fishman, J., 1981. The distribution of carbon monoxide and ozone in the free troposphere. J. Geophys. Res. 86, 7255–7265.

Tuck et al, A., F, , 1997. The Brewer–Dobson circulation in the light of high altitude *in situ* aircraft observations. Quart. J. Roy. Met. Soc. 123, 1–69.

Waibel, A.E., Fischer, H., Siegmund, P.C., Lee, B., Wienhold, F.G., Crutzen, P.J., Lelieveld, J., Strom, J., 1998. Highly elevated carbon monoxide concentrations in the upper troposphere and lowermost stratosphere at northern mid-latitudes during STREAM II summer campaign in 1994. Chemosphere, this issue.

Waugh, D.W., 1996. Seasonal variation of isentropic transport out of the tropical stratosphere. J. Geophys. Res. 101, 4007–4023.

Webster, C.R., May, R.D., Trimble, C.A., Chave, R.G., Kendall, J., 1994. Aircraft (ER-2) laser infrared absorption spectrometer (ALIAS) for in situ stratospheric measurements of HCl, N_2O, CH_4, NO_2 and HNO_3. Appl. Opt. 33, 454–472.

Weinstock, E.M., Hintsa, E.J., Anderson, J.G., Boering, K.A., Daube, B.C., Wofsy, S.C., Herman, R.L., May, R.D., Webster, C.R., Bui, T.P., 1999. Evaluation of the seasonal cycle of water vapor in the stratosphere from monthly average tropical tropopause temperatures using a CO photochemical clock. J. Geophys. Res., submitted.

Weinstock, E.M., Hintsa, E.J., Dessler, A.E., Oliver, J.F., Hazen, N.L., Demusz, J.N., Allen, N.T., Lapson, L.B., Anderson, J.G., 1994. A new fast response photofragment fluorescence hygrometer for use on the NASA ER-2 and Perseus remotely piloted aircraft. Rev. Sci. Instrum. 65, 3544–3554.

Wennberg, P.O., Cohen, R.C., Hazen, N.L., Lapson, L.B., Allen, N.T., Hanisco, T.F., Oliver, J.F., Lanham, N.W., Demusz, J.N., Anderson, J.G., 1994. Aircraft-borne, laser-induced fluorescence instrument for the in situ detection of hydroxyl and hydroperoxyl radicals. Rev. Sci. Instrum. 65, 1858–1876.

Yurganov, L.N., Jaffe, D.A., Pullman, E., Novelli, P.C., 1998. Total column and surface densities of atmospheric carbon monoxide in Alaska, 1995. J. Geophys. Res. 103, 19337–19346.

Dr. Robert L. Herman is currently a postdoctoral scholar in the Atmospheric Laser Spectroscopy Group at the Jet Propulsion Laboratory in Pasadena, California. He received his Ph.D. in geochemistry from the California Institute of Technology in 1998, studying under Prof. Yuk L. Yung and Dr. Chris R. Webster of Jet Propulsion Laboratory, with a thesis entitled "In situ measurements of chemical tracers in the stratosphere: CO, N_2O, and CH_4." His research interests include stratospheric chemistry and dynamics, tunable diode lasers, infrared spectroscopy of gases, and Raman spectroscopy of minerals.